Available online at www.sciencedirect.com
SCIENCE DIRECT®
Journal of Photochemistry and Photobiology A: Chemistry 157 (2003) 301–309
Journal of Photochemistry and Photobiology A:Chemistry
www.elsevier.com/locate/jphotochem

Rate constants for the photolysis of the nitronaphthalenes and methylnitronaphthalenes

Patricia T. Phousongphouang [a], Janet Arey [a,b,*]

[a] Environmental Toxicology Graduate Program and Air Pollution Research Center, University of California, Riverside, CA 92521, USA
[b] Department of Environmental Sciences, University of California, Riverside, CA 92521, USA

Received 30 May 2002; received in revised form 14 September 2002; accepted 14 September 2002

Abstract

1-Nitronaphthalene (1NN) and 2-nitronaphthalene (2NN) are among the most abundant gas-phase nitro-polycyclic aromatic hydrocarbons (nitro-PAHs) found in ambient atmospheres, largely formed from the atmospheric reactions of naphthalene. The methylnitronaphthalenes (MNNs), of which there are 14 possible isomers, are gas-phase atmospheric transformation products of 1- and 2-methylnaphthalene. In this investigation, the photolysis rates of 1NN, 2NN, and 11 MNNs were determined indoors using black-lamp irradiation and outdoors using natural sunlight. The results of the photolysis experiments reveal that gas-phase photolysis is a major atmospheric degradation pathway for the NNs and MNNs. The nitro-PAHs examined here can be placed into three groups on the basis of their expected lifetimes due to ambient photolysis. 1M8NN and 2M1NN are predicted to have ambient lifetimes toward photolysis of ≤15 min; 1NN, 1M2NN, 1M4NN, 1M5NN, 2M4NN, 2M5NN, 2M8NN are predicted to have photolysis lifetimes ≤1 h; and 2NN, 2M6NN, 1M6NN and 1M3NN are predicted to have lifetimes on the order of 1–3 h. Thus, photolysis is expected to be the dominant atmospheric loss process for these volatile nitro-PAHs.

Keywords: Gas-phase; Kinetics; Methylnitronaphthalenes; Nitronaphthalenes; Nitro-PAH; Photolysis

1. Introduction

The nitronaphthalenes, 1NN and 2NN, and the 14 methylnitronaphthalenes (1M*x*NN and 2M*x*NN) are 2-ring nitro-polycyclic aromatic hydrocarbons (nitro-PAHs) found in the gas-phase in ambient atmospheres [1,2]. Reported at levels up to several nanograms per cubic meter, 1- and 2NN are the most abundant individual airborne nitro-PAHs, and the sum of their methyl-derivatives have been observed at similar levels [2–5]. The NNs have been found to be genotoxic in vitro [5–12] and in vivo [13,14] and recently 1NN has been shown to produce acute lung injury in vivo [15–17]. While fewer toxicity results on the MNNs are available, they have been observed to be bacterial mutagens in the *Salmonella typhimurium* assay and to account for a significant fraction of ambient air mutagenicity measured employing this assay [5].

Sources for the NNs and MNNs in ambient air include atmospheric formation from the parent naphthalene or methylnaphthalenes [3,18,19] and emissions from combustion sources such as diesel exhaust [20–24]. Atmospheric NN and MNN formation occurs through daytime reaction of the gas-phase parent PAH with the hydroxyl (OH) radical and nighttime reaction with the nitrate (NO_3) radical, each in the presence of NO_x. In the laboratory, the OH radical-initiated reactions form nitro-PAH in low yields (∼3% NNs from naphthalene, <1% MNNs from 1MN or 2MN) [3,18,19]. In contrast the yields from the NO_3 radical-initiated reactions are high (∼35% NNs from naphthalene, ∼30% MNNs from 1MN or 2MN) [3,18,19].

Distinct isomer profiles of the MNNs are formed from each of the radical-initiated reactions, which differ from the major electrophilic nitration products that generally appear in combustion emissions. For example, 1M5NN, 1M6NN and 1M4NN are prominently formed from the OH radical reaction while 2M4NN dominates from NO_3 radical formation [3,4], and 2M1NN has been reported in diesel exhaust [21]. Ambient air data of MNN profiles from throughout California suggest that atmospheric formation of these 2-ring nitro-PAHs dominates over direct emission [3–5,25]. Furthermore, while daytime OH radical reaction is ubiquitous and this reaction is expected to be the major loss process for atmospheric naphthalene and MNs, the high yield of nitro-PAHs from the nighttime NO_3 radical reaction can result in this reaction dominating nitro-PAH formation. Thus,

* Corresponding author. Tel.: +1-909-787-3502; fax: +1-909-787-5004.
E-mail address: janet.arey@ucr.edu (J. Arey).

1010-6030/03/$ – see front matter © 2003 Elsevier Science B.V. All rights reserved.
doi:10.1016/S1010-6030(03)00072-8

ambient MNN profiles resulting from daytime OH radical formation were reported at Torrance [26], Glendora [2] and Azusa, CA [27], while nighttime MNN profiles indicating the dominance of NO_3 radical formation were measured during photochemical pollution episodes at Redlands [4,5] and Banning, CA [27], sites downwind of metropolitan Los Angeles.

In addition to knowledge of their atmospheric formation, modeling of the atmospheric concentrations of nitro-PAHs will require knowledge of their atmospheric loss processes. Studies of the atmospheric chemistry of volatile nitro-PAHs including 1NN, 2NN and 2M1NN suggest that photolysis and/or reaction with the OH radical will be their major atmospheric loss process(es), while reaction with the NO_3 radical and O_3 are expected to be of negligible importance [28–30]. In this work, we re-investigate the photolysis of the NNs and 2M1NN and examine the photolysis of 10 other MNN isomers (1M2NN, 1M3NN, 1M4NN, 1M5NN, 1M6NN, 1M8NN, 2M4NN, 2M5NN, 2M6NN, and 2M8NN). The photolysis reaction rates have been examined both indoors using black-lamp irradiation and outdoors with irradiation by natural sunlight.

2. Experimental

2.1. Synthesis of the methylnitronaphthalenes

The 1MNNs and 2MNNs were synthesized as described previously [4,31] by nitrating the parent 1- or 2MN with dinitrogen pentoxide (N_2O_5) in carbon tetrachloride solution at room temperature. Prior to its use, the 2MN was purified by re-crystallization, resulting in a purity of 99%. The specific MNN isomers formed were identified by matching their gas chromatographic retention times and mass spectra with those previously obtained for authentic standards of each of the 14 MNNs [4,32]. The MNN product distributions were as follows: from 1MN nitration; 1M2NN (9%), 1M3NN (8%), 1M4NN (48%), 1M5NN (23%), 1M6NN (2%), 1M8NN (10%) and from 2MN nitration; 2M1NN (40%), 2M4NN (25%), 2M5NN (13%), 2M6NN (2%), 2M8NN (20%). Thus, the nitrations formed 11 of the 14 MNNs and because gas chromatography with flame ionization detection (GC-FID) analysis was employed for quantification, the synthesized 1MNNs and 2MNNs were used without further purification.

2.2. Indoor photolysis

Experiments were carried out as described previously [29] in a 7000-L indoor all-Teflon chamber at 298 ± 2 K and 740 Torr total pressure of purified air at ~5% relative humidity. The chamber is equipped with two parallel banks of black-lamps for irradiation and a Teflon-coated fan to ensure rapid mixing of reactants during their introduction into the chamber. Compounds were introduced into the chamber by flushing ultrahigh-purity nitrogen gas through a heated Pyrex bulb containing one of three mixtures: (1) 1NN, 2NN, and 2M1NN; (2) 1NN and the synthesized 1MNN isomers; or (3) 1NN and the synthesized 2MNN. Also added to the chamber were cyclohexane, in excess, to serve as an OH radical scavenger and tetradecane as a reference compound for determining retention indices.

The nitro-PAHs were photolyzed in three batches containing the following individual nitro-PAH, with their approximate initial concentrations (in molecules cm^{-3}) listed after each compound: *batch 1*, 1NN, $(2.0–4.0) \times 10^{11}$; 2NN, $(1.6–2.7) \times 10^{11}$; 2M1NN, $(3.2–6.8) \times 10^{11}$; *batch 2*, 1NN, $(1.0–19) \times 10^{11}$; 1M2NN, $(0.56–2.0) \times 10^{11}$; 1M3NN, $(0.36–0.78) \times 10^{11}$; 1M4NN, $(3.3–8.0) \times 10^{11}$; 1M5NN, $(1.1–4.2) \times 10^{11}$; 1M6NN, $(0.11–0.13) \times 10^{11}$; 1M8NN, $(0.34–4.4) \times 10^{11}$; and *batch 3*, 1NN, $(6.3–38) \times 10^{11}$; 2M1NN, $(7.2–38) \times 10^{11}$; 2M4NN, $(1.1–10.5) \times 10^{11}$; 2M5NN, $(0.46–4.2) \times 10^{11}$; 2M6NN, $(0.09–0.31) \times 10^{11}$; 2M8NN, $(1.1–7.3) \times 10^{11}$. Also added prior to photolysis of each nitro-PAH batch were cyclohexane and tetradecane at 5.3×10^{13} and 3.3×10^{11} molecules cm^{-3}, respectively.

For each experiment, before irradiation was started, the sampling port was conditioned by establishing a small flow from the chamber (this flow was continued throughout the reaction between samples) and two to three replicate samples were collected and analyzed to establish the initial nitro-PAH concentrations. The concentrations of reactants were monitored during these experiments by GC-FID analysis of 1.0 l samples collected onto Tenax-TA solid adsorbent cartridges at a flow rate of 100 ml min^{-1} using a pump and mass flow controller (Tylan General). The samples were subsequently thermally desorbed in the injection port of the GC inlet at 280 °C onto a 30 m DB-5MS megabore column and/or a 30 m DB-1701 column held at 40 °C for 10 min and then temperature-programmed to 160 °C at 20 °C min^{-1}, then to 200 °C at 4 °C min^{-1} and then to 280 °C at 20 °C min^{-1}.

For each experiment, five 15 min irradiations of the nitro-PAHs were carried out at 20% light intensity (corresponding to a measured NO_2 photolysis rate, J_{NO_2}, of 0.114 min^{-1}) with a Tenax sample(s) being taken for analysis after each irradiation interval. Replicate irradiation experiments were conducted as follows: *batch 1*, three replicates performed with analyses on the DB-5MS column; *batch 2*, three replicates performed with analyses on the DB-5MS column and two replicates performed with analyses on the DB-1701 column; and *batch 3*, three replicates performed with analyses on the DB-5MS column and two replicates performed with analyses on the DB-1701 column.

2.3. Outdoor photolysis

The outdoor photolysis experiments were conducted with natural sunlight on days that were clear and sunny with outdoor temperatures ranging from 18 to 27 °C. The irradiations were conducted at ground level on a grass surface between 11:30 and 12:30 PST. Measurements of J_{NO_2} were carried

out periodically using the quartz tube method of Zafonte et al. [33] and gave a J_{NO_2} of 0.274 ± 0.07 (2σ; $n = 46$).

Experiments were carried out in a 4000 l outdoor Teflon chamber equipped with a Teflon-coated fan to ensure rapid mixing of reactants during their introduction into the chamber. The nitro-PAHs were introduced into the chamber by flushing ultrahigh-purity nitrogen gas through a heated Pyrex U-tube containing glass beads coated with one of the three nitro-PAH mixtures noted above. Cyclohexane and tetradecane were added to the chamber from a heated bulb at concentrations of 9.2×10^{13} and 5.8×10^{11} molecules cm^{-3}, respectively. The chamber was covered with a reflective tarpaulin during the approximately 10–20 min required to flush the compounds into the chamber.

In contrast to the indoor experiments where photolysis could readily be stopped by turning off the black lamps, covering the chamber was required to stop photolysis in the outdoor experiments and this resulted in temperature increases which led to wall desorption problems. Therefore, once the outdoor chamber was uncovered, the irradiation and sampling were continuous. Ten minutes prior to uncovering the chamber, pumping was initiated to condition the sampling port and once the chamber was uncovered, the first sample was started after 10 min (to allow the chamber temperature to equilibrate). During irradiation, 4 l gas-phase samples were collected consecutively over a 1 h time period onto Tenax-TA solid adsorbent cartridges at a flow rate of 400 ml min^{-1} using a pump and mass flow controller (Tylan General). The samples were subsequently thermally desorbed and analyzed by GC-FID as described above.

The same nitro-PAH batches were utilized for the outdoor experiments as indoors. The individual nitro-PAHs and their "initial" concentrations, as sampled beginning 10 min after the chamber was uncovered, are listed after each compound (in molecules cm^{-3}): *batch 1*, 1NN, (0.09–4.2) $\times 10^{11}$; 2NN, (0.10–52) $\times 10^{11}$; 2M1NN, (0.11–3.6) $\times 10^{11}$; *batch 2*, 1NN, (0.14–4.2) $\times 10^{11}$; 1M2NN, (0.11–2.0) $\times 10^{11}$; 1M3NN, (0.02–1.7) $\times 10^{11}$; 1M4NN, (0.04–7.8) $\times 10^{11}$; 1M5NN, (0.03–2.3) $\times 10^{11}$; 1M6NN, (0.03–0.28) $\times 10^{11}$; 1M8NN, (0.05–1.7) $\times 10^{11}$; and *batch 3*, 1NN, (3.2–9.1) $\times 10^{11}$; 2M1NN, (0.65–5.4) $\times 10^{11}$; 2M4NN, (0.14–2.5) $\times 10^{11}$; 2M5NN, (0.22–0.78) $\times 10^{11}$; 2M6NN, (0.04–0.16) $\times 10^{11}$; 2M8NN, (0.47–1.7) $\times 10^{11}$. Replicate irradiations were conducted as follows: *batch 1*, two replicates performed with analyses on the DB-5MS column and eight replicates performed with analyses on the DB-1701 column; *batch 2*, three replicates performed with analyses on the DB-5MS column and nine replicates performed with analyses on the DB-1701 column; and *batch 3*, one replicate performed with analyses on the DB-5MS column and four replicates performed with analyses on the DB-1701 column.

2.4. Chemicals

The chemicals used, and their stated purities, were carbon tetrachloride (>99%, anhydrous), 1MN (99%), 2MN (98%), 2M1NN (99%), 1NN (99%), 2NN (98%), and tetradecane (99%), purchased from Aldrich Chemical Co. (Milwaukee, WI); cyclohexane (HPLC grade) and methylene chloride (OPTIMA), purchased from Fisher Scientific (Tustin, CA).

3. Results and discussion

A series of nitro-PAH–tetradecane–cyclohexane–air irradiations were carried out indoors using black-lamp irradiation and outdoors under natural sunlight. In general:

$$\ln\left\{\frac{[\text{nitro-PAH}]_{t_0}}{[\text{nitro-PAH}]_t}\right\} = k_{\text{phot}}(t - t_0) \quad (1)$$

where $[\text{nitro-PAH}]_{t_0}$ is the concentration of the nitro-PAH at time t_0, $[\text{nitro-PAH}]_t$ the corresponding concentration at time t, and k_{phot} is the rate constant for the following reaction:

$$\text{nitro-PAH} + h\nu \rightarrow \text{products} \quad \text{(photolysis)}$$

Therefore, plots of $\{\ln([\text{nitro-PAH}]_{t_0}/[\text{nitro-PAH}]_t)\}$ against $(t - t_0)$ should be straight lines with a slope of k_{phot} and a zero intercept.

The observed rate constants for both the indoor and outdoor photolysis experiments are presented in Table 1, and representative plots of Eq. (1) are shown in Figs. 1 and 2. As seen in Figs. 1 (upper panel) and 2, results from the indoor photolysis experiments produced the anticipated linear plots, while the photolysis outdoors (Fig. 1, lower panel) gave curved plots.

The upper panel of Fig. 1 shows the results for the indoor photolysis of the NNs and 2M1NN (batch 1). Reproducible pre-irradiation values were obtained for the NNs and MNNs in the indoor 7000 l chamber, suggesting that dark wall losses were negligible. Furthermore, the decays were linear, for example, for up to 90% reaction of 2M1NN (see Fig. 1, upper panel), indicating that desorption from the chamber walls as the gas-phase concentration decreased was not occurring.

In order to obtain good data for the less abundant MNN isomers in the synthesized mixtures, the concentrations of some of the MNN isomers were greater than those used for batch 1. 1NN was present in all three nitro-PAH batches and 2M1NN was present in batches 1 and 3. The compounds at the highest initial concentrations ($\sim 40 \times 10^{11}$ molecules cm^{-3}) were 1NN and 2M1NN and photolysis rate data obtained for these compounds were batch independent, indicating a lack of wall adsorption/desorption problems for these indoor experiments.

Initial experiments with a 1500 l Teflon chamber outdoors showed clear evidence of nitro-PAH partitioning to and from the walls. In an attempt to overcome these problems the chamber size was increased to 4000 l and rather than photolysis followed by dark periods, continuous irradiation was done to avoid heating of the chamber when covered. As noted, the samples that were collected starting at 10 min after the chamber was uncovered were taken as the "initial"

Table 1
Measured photolysis rates, k_{phot}, in a 7000 l indoor all-Teflon chamber and a 4000 l outdoor all-Teflon chamber with calculated atmospheric lifetimes

	$10^3 \times k_{phot}$ (min^{-1})		Calculated lifetime, τ (min)	
	Indoor[a] ($J_{NO_2} = 0.114\,min^{-1}$)	Outdoor[b] ($J_{NO_2} = 0.274\,min^{-1}$)	Indoor ($J_{NO_2} = 0.312\,min^{-1}$)	Outdoor ($J_{NO_2} = 0.312\,min^{-1}$)
1NN	15.1 ± 1.7	50 ± 21	24	18
2NN	2.1 ± 0.6	12 ± 16	177	73
1M2NN	11.6 ± 2.7	27 ± 25	31	33
1M3NN[c]	5.2 ± 2.0	20 ± 19	71	44
1M4NN[d]	16.7 ± 3.7	63 ± 27	22	14
1M5NN	9.6 ± 3.2	40 ± 35	38	22
1M6NN[e]	4.2 ± 1.0	8 ± 30	88	110
1M7NN[f]	nd	nd	nd	nd
1M8NN	61.7 ± 23.1	73 ± 99	6	12
2M1NN	36.7 ± 4.5	103 ± 31	10	9
2M3NN[f]	nd	nd	nd	nd
2M4NN	8.8 ± 3.0	41 ± 10	41	21
2M5NN	7.5 ± 3.2	49 ± 15	49	18
2M6NN	2.8 ± 4.0	3 ± 54	133	293
2M7NN[f]	nd	nd	nd	nd
2M8NN	11.7 ± 2.7	38 ± 11	31	23

[a] Indicated errors are two least-squares standard deviations.
[b] The k_{phot} values are obtained from the initial slopes of second-order linear regressions. Indicated errors are two least-squares standard deviations obtained from the initial set of data points at an irradiation time of 10–12 min and may overestimate the uncertainties.
[c] 1M3NN was resolved on the DB-1701 GC column from other 1MNN isomers, although interference from non-MNN species produced in the synthesis cannot be ruled out. On the DB-5 GC column, 1M3NN co-elutes with 1M7NN; however the peak represents primarily the 1M3NN isomer since 1M7NN is not obtained in significant amounts from the solution-phase synthesis [3,5] and no correction was made for the presence of 1M7NN.
[d] On the DB-1701 GC column, 1M4NN and 1M7NN co-eluted, but no correction was made for the presence of 1M7NN (see footnote c). On the DB-5 GC column, 1M4NN co-elutes with 1M6NN, but the amount of 1M6NN was shown to be small from the analysis on the DB-1701 GC column and no correction was made.
[e] 1M6NN was well resolved on the DB-1701 column, but co-elutes with 1M4NN on the DB-5 GC column as stated above. The photolysis rate listed was obtained from the data analysis performed on the DB-1701 GC column.
[f] Synthesis produced insufficient yields to allow measurements, therefore measurements were not determined (nd).

concentrations. As evident from Fig. 1 (lower panel), as the reaction proceeded desorption from the walls decreased the apparent decay rate. This is consistent with the conclusion of Feilberg et al. that evaporation of NNs from particles was fast enough to keep up with the gas-phase photolysis decay [24,34]. Therefore, to determine k_{phot} outdoors the initial slopes of second-order linear regressions were used.

The experimentally determined NO_2 photolysis rate, J_{NO_2}, for the indoor photolysis experiments was 0.114 min^{-1}, a factor of 2.4 lower than the average outdoor value of $J_{NO_2} = 0.274 \pm 0.077\,min^{-1}$. Taking the difference in light intensity into account, the indoor and outdoor measurements overlap within the uncertainties stated in Table 1 for all the nitro-PAHs except 2M4NN and 2M5NN, where the indoor photolysis rate measurements are lower. Considering the large uncertainties in the outdoor measurements and the overall consistency of the measurements, for example, the fastest rates are for 1M8NN, 2M1NN, 1M4NN and 1NN and the slowest for 2NN, 2M6NN and 1M6NN for both the indoor and outdoor photolysis experiments, the indoor measurements are preferred and, when referenced to the appropriate J_{NO_2}, are taken to be predictive of photolysis under natural sunlight conditions.

Compared in Table 2 are the present results and those previously reported for the NNs from this laboratory [28] and by Feilberg et al. [24,34] and the values previously reported from this laboratory for 2M1NN [29]. As noted, the indoor and outdoor measurements described here are in agreement for 1NN, 2NN and 2M1NN and are in general agreement with the indoor values reported from this laboratory over 10 years ago. At that time, shorter photolysis times at higher light intensities were employed and only an upper limit for the photolysis rate was determined for 2NN, which was noted to initially increase by 10–20% after

Table 2
Measured photolysis rates, k_{phot}, indoors and outdoors

	$10^3 \times k_{phot}$ (min^{-1})[a]		
	Indoor	Outdoor	Reference
1NN	41 ± 5	57 ± 24	This work
	64 ± 5	9.9 ± 0.8	Atkinson et al. [28]
		22	Feilberg et al. [24]
2NN	5.7 ± 1.6	14 ± 19	This work
	≤8	7.7 ± 0.6	Atkinson et al. [28]
		2	Feilberg et al. [24]
2M1NN	100 ± 13	117 ± 36	This work
	148 ± 28	8.0 ± 2.2	Arey et al. [29]

[a] Indicated errors are two least-squares standard deviations. Calculated for $J_{NO_2} = 0.312\,min^{-1}$.

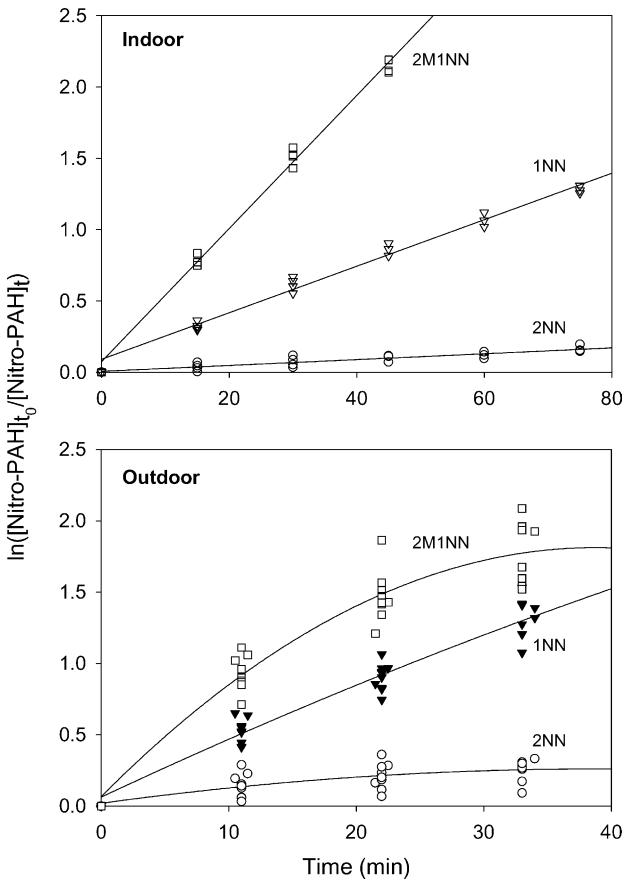

Fig. 1. Plots of Eq. (1) for the gas-phase photolysis of 2NN, 1NN, and 2M1NN (batch 1) in an indoor chamber with black-lamp irradiation and in an outdoor chamber with sunlight irradiation. The results from three replicate experiments conducted indoors are shown in the upper panel (the fourth points at 15 and 30 min are replicate samples). For the indoor photolysis, the k_{phot} at $J_{NO_2} = 0.114\,min^{-1}$ are $(2.06 \pm 0.53) \times 10^{-3}$, $(16.3 \pm 1.1) \times 10^{-3}$, and $(46.6 \pm 2.5) \times 10^{-3}$, for 2NN, 1NN, and 2M1NN, respectively. These indoor results for 1NN and 2M1NN are a subset of the complete data set used to calculate the values given in Table 1. The results from 10 replicate experiments conducted outdoors are shown in the lower panel with a second-order linear regression plot. The k_{phot} at $J_{NO_2} = 0.274\,min^{-1}$ taken from the initial slopes are $(12 \pm 16) \times 10^{-3}$, $(50 \pm 21) \times 10^{-3}$, and $(103 \pm 31) \times 10^{-3}$ for 2NN, 1NN, and 2M1NN, respectively. Note that the concentrations measured for samples begun 10 min after the chamber was uncovered were used for the zero time values in these outdoor experiments.

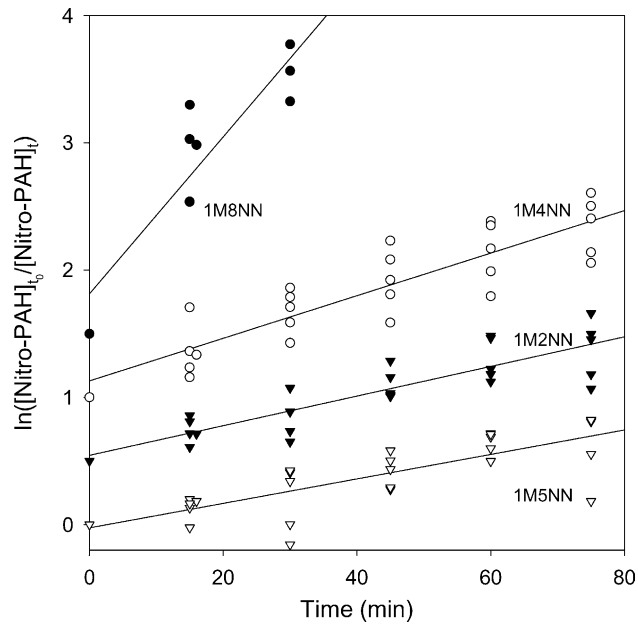

Fig. 2. Plots of Eq. (1) for the gas-phase photolysis of 1M5NN, 1M2NN, 1M4NN, and 1M8NN in an indoor chamber with black-lamp irradiation, where k_{phot} at $J_{NO_2} = 0.114\,min^{-1}$ are $(9.62 \pm 3.19) \times 10^{-3}$, $(11.6 \pm 2.7) \times 10^{-3}$, $(16.7 \pm 3.7) \times 10^{-3}$, and $(61.7 \pm 23.1) \times 10^{-3}$, respectively. The data for 1M2NN, 1M4NN, and 1M8NN have been displaced vertically by 0.5, 1.0, and 1.5 units, respectively, for clarity.

turning on the lights. At 20% light intensity as used here for the indoor experiments, temperature variations due to heating of the chamber and potential wall adsorption/desorption of the nitro-PAHs should be minimized. In the previous outdoor experiments, initial increases in concentration during the first 5 min of photolysis were noted, followed by linear decreases, which were much slower than observed indoors for 1NN and 2M1NN [28,29]. It is now believed that the decreases were dominated by wall adsorption/desorption processes in the small chamber ($1\,m^3$) employed at that time.

In agreement with our present values, the photolysis of 1NN was much faster than that of 2NN as measured by Feilberg et al. in a very large ($190\,m^3$) outdoor Teflon chamber, in the presence of $0.8\,mg\,m^{-3}$ of diesel exhaust particles [24,34]. It is not known if the presence of the particles resulted in the factor of ∼2 slower photolysis of the NNs observed by Feilberg et al. [24,34].

Gas-phase absorption spectra of the MNNs are not available, but using the reported absorption cross-sections for 2M1NN in ethanol solution and a Tropospheric Ultraviolet Model (TUV model version 4.0), an effective quantum yield of 3.5×10^{-3} has been calculated [35] based on the previously reported [29] outdoor photolysis rate for 2M1NN (see Table 2). Employing the 2M1NN photolysis rate reported here, the resulting quantum yield for 2M1NN would be $\sim 4 \times 10^{-2}$.

The photochemistry of nitroaromatic compounds has been attributed to intramolecular nitro to nitrite rearrangements [36–39]. The photochemistry of the nitropyrenes (NP) has been described as resulting from the interaction of the nitro group with the aromatic π system of pyrene, with 1NP, where the interaction is strong, undergoing photolysis much more rapidly than 2NP. The photochemistry was shown to correlate with the electron impact mass-spectroscopic properties of the NPs in that 1NP shows a strong $[M–NO]^+$ fragment attributed to NO_2 to ONO rearrangement followed by loss of NO from the molecular ion, and this fragment is lacking in the spectrum of 2NP. Furthermore, the identification of 1-hydroxy-2-nitropyrene from 1NP photolysis suggested intramolecular rearrangement of the excited state to form 1-hydroxy-2-nitrosopyrene, which is readily oxidized [38].

The much faster photolysis of 1NN relative to 2NN suggests that the slow photolysis of 2NN is attributable to little interaction of the nitro group with the naphthalene π aromatic system, consistent with the lack of an $[M–NO]^+$ fragment in the mass spectra of 2NN [40,41]. Although 1NN eliminates CO from the molecular ion through a mechanism that has been shown not to involve nitro to nitrite rearrangement [40], in collision-induced dissociation spectra, 1NN shows the loss of NO to be the major fragmentation above 58 eV, with CO loss dominating at 20 eV [42]. The formation of 1-hydroxy-2-nitronaphthalene from the photolysis of gas-phase 1NN has been observed [28], supporting intramolecular rearrangement in 1NN photolysis.

Table 3 lists the NNs and MNNs with nitro substitution on C_1 and C_2 of naphthalene according to their photolysis rates. It can be observed that all the compounds with NO_2 on C_1 are more reactive than the compounds with NO_2 on C_2, with the exception of 1M2NN, which has an *ortho* methyl group. Those isomers with NO_2 on the C_1 are somewhat non-planar, with the NO_2 forced out of the plane by the *peri* hydrogen [43] and these photolyze more rapidly than the planar isomers. For 1M8NN, the NO_2 and the methyl group are *peri* to one another and 1M8NN is most rapidly photolyzed. The slowest photolysis occurs for 2NN, 2M6NN, 1M6NN, and 1M3NN, all planar molecules with the NO_2 on the C_2 carbon. Only for 1M2NN, where the *ortho* methyl groups forces the NO_2 out of the plane of the naphthalene ring system, is the photolysis comparable to isomers with the NO_2 on C_1.

The non-planar nature of the nitronaphthalenes with methyl substituents *ortho* or *peri* to the nitro group is

Table 3
Nitronaphthalenes and methylnitronaphthalenes with NO_2 substitution on C_1 and NO_2 substitution on C_2 listed according to photolysis rate[a]

NO_2	Photolysis rate	NO_2 on C_2	Photolysis rate
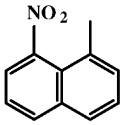 1M8NN	62	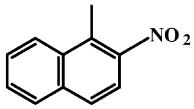 1M2NN	12
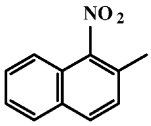 2M1NN	37	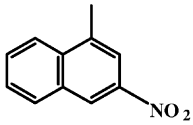 1M3NN	5
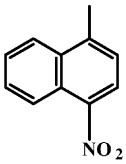 1M4NN	17	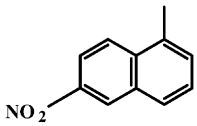 1M6NN	4
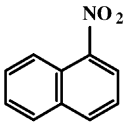 1NN	15	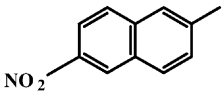 2M6NN	3
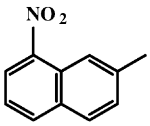 2M8NN	12	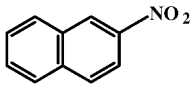 2NN	2
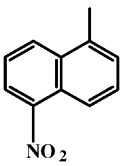 1M5NN	10		
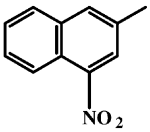 2M4NN	9		
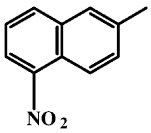 2M5NN	7		

[a] Photolysis rate is $10^3 \times k_{phot}$ (min^{-1}) measured indoors at $J_{NO_2} = 0.114\,min^{-1}$.

suggested by their NMR spectra which show evidence for steric crowding in the diminished downfield shifts of the protons *ortho* to the nitro groups in 1M2NN and 1M8NN and of the *peri* proton in 2M1NN [4,44] relative to the NNs. Also the mass spectra of these MNNs show an $[M–OH]^+$ fragment [4,32], which has been noted as characteristic of nitro-PAHs containing a sterically hindered nitro group [38]. Presumably nitro group orientations that favor intramolecular rearrangement of the excited state will photolyze most rapidly [37–39]. However, it has been shown that non-planarity alone does not result in rapid photolysis. 1-Methyl-2-nitropyrene (1M2NP) is expected to be non-planar with the methyl group at position 1 forcing the nitro group at position 2 out of the plane and, indeed the spectroscopic evidence confirms this [38], but 1M2NP is, like 2NP, very stable towards light [38]. The corresponding isomer in the naphthalene system, 1M2NN, is the most reactive of the isomers with the NO_2 on C_2, but is significantly less reactive than 2M1NN toward photolysis.

Both the NNs and MNNs have been found to contribute significantly to ambient gas-phase mutagenicity [5], therefore, it is important to study the effects of photolytic decay of nitro-PAHs and their fate in the environment in order to predict the risk to human health. Based on the photolysis rates determined both indoors using black-lamp irradiation and outdoors using natural sunlight, the lifetimes of these compounds have been determined using a 12 h ambient average J_{NO_2} of 0.312 min^{-1} (see Table 1). The nitro-PAHs examined here can be placed into three groups on the basis of their expected lifetimes due to ambient photolysis. 1M8NN and 2M1NN are expected to have ambient lifetimes toward photolysis of $\leq$15 min; 1NN, 1M2NN, 1M4NN, 1M5NN, 2M4NN, 2M5NN, 2M8NN are expected to have photolysis lifetimes $\leq$1 h; and 2NN, 2M6NN, 1M6NN and 1M3NN are predicted to have lifetimes on the order of 1–3 h. Thus, photolysis is expected to be the dominant atmospheric loss process for these volatile nitro-PAHs. Reaction with the OH radical has been examined for the NNs and the lifetimes estimated at ~2 days [28]. The addition of a methyl substituent to the NN will increase the OH radical reaction rates, but this methyl activation is expected to be only about a factor of 2.6 [45], consistent with the previously reported upper limit to the rate constant for 2M1NN [29].

Little empirical data are available for the vapor pressures of nitro-PAHs, but the vapor pressures of the NNs and MNNs have been calculated to be similar to that of phenanthrene [46]. At 25 °C and 100 $\mu g\,m^{-3}$ aerosol concentration, phenanthrene is calculated to be 3% in the aerosol phase [47] and the NNs and MNNs are also expected to be predominantly in the gas-phase. At low ambient temperatures and/or with very high particle loadings, the NNs and MNNs may distribute into the particle phase, but under most conditions encountered in temperate areas the NNs and MNNs will be mainly in the gas-phase in the troposphere [1,2,26,46] and loss to particles is not expected to compete with photolysis as a tropospheric loss process for these compounds.

The photolysis rates measured here have interesting toxicological implications. 2NN has a longer lifetime due to photolysis than does 1NN, and is also more mutagenic in *Salmonella* [5,10]. For the MNNs, the same factors which result in shorter photolysis lifetimes, methyl substitution *ortho* to the nitro group and nitro group substitution on C_1, result in lower mutagenic activity [4,5,8]. Therefore, for the volatile nitro-PAHs examined here, the longer-lived species are also more mutagenic.

Acknowledgements

The authors thank Roger Atkinson, University of California, Riverside, for helpful discussions, and William D. Long, University of California, Riverside, for his ingenious problem solving. The authors would also like to thank the Department of Energy Contract no. DE-FG03-01-ER-63095, for supporting this research. While this research was supported by the Department of Energy, it has not been subjected to Agency review and therefore does not necessarily reflect the views of the Agency and no official endorsement should be inferred.

References

[1] R.W. Coutant, L. Brown, J.C. Chuang, R.M. Riggin, R.G. Lewis, Phase distribution and artifact formation in ambient air sampling for polynuclear aromatic hydrocarbons, Atmos. Environ. 22 (1988) 403–409.

[2] J. Arey, R. Atkinson, B. Zielinska, P.A. McElroy, Diurnal concentrations of volatile polycyclic aromatic hydrocarbons and nitroarenes during a photochemical air pollution episode in Glendora, California, Environ. Sci. Technol. 23 (1989) 321–327.

[3] B. Zielinska, J. Arey, R. Atkinson, P.A. McElroy, Formation of methylnitronaphthalenes from the gas-phase reactions of 1- and 2-methylnaphthalene with OH radicals and N_2O_5 and their occurrence in ambient air, Environ. Sci. Technol. 23 (1989) 723–729.

[4] P. Gupta, The contribution of methylnitronaphthalenes to the vapor-phase mutagenicity observed in ambient air samples collected at Redlands, California, M.Sc. Thesis in Environmental Toxicology, March 1995, University of California, Riverside, p. 263.

[5] P. Gupta, W.P. Harger, J. Arey, The contribution of nitro- and methylnitronaphthalenes to the vapor-phase mutagenicity of ambient air samples, Atmos. Environ. 30 (1996) 3157–3166.

[6] V.F. Simmon, In vitro mutagenicity assays of chemical carcinogens and related compounds with *Salmonella typhimurium*, J. Natl. Cancer Inst. 62 (1979) 893–899.

[7] R.J. Pienta, Evaluation and relevance of the Syrian hamster embryo cell system, in: G.M. Williams, R. Kroes, H.W. Waaijers, K.W. van de Poll (Eds.), The Predictive Value of Short-term Screening Tests in Carcinogenicity Evaluation, Elsevier, Amsterdam, 1980, pp. 149–169.

[8] K. El-Bayoumy, E.J. Lavoie, S.S. Hecht, E.A. Fow, D. Hoffman, The influence of methyl substitution on the mutagenicity of nitronaphthalenes and nitrobiphenyls, Mutat. Res. 81 (1981) 143–153.

[9] H. Tokiwa, Y. Ohnishi, Mutagenicity and carcinogenicity of nitroarenes and their sources in the environment, CRC Crit. Rev. Toxicol. 17 (1986) 23–60.
[10] J. Arey, W.P. Harger, D. Helmig, R. Atkinson, Bioassay-directed fractionation of mutagenic PAH atmospheric photooxidation products and ambient particulate extracts, Mutat. Res. 281 (1992) 67–76.
[11] J.C. Sasaki, J. Arey, D.A. Eastmond, K.K. Parks, A.J. Grosovsky, Genotoxicity induced in human lymphoblasts by atmospheric reaction products of naphthalene and phenanthrene, Mutat. Res. 393 (1997) 23–35.
[12] J.C. Sasaki, J. Arey, D.A. Eastmond, K.K. Parks, P.T. Phousongphouang, A.J. Grosovsky, Evidence for oxidative metabolism in the genotoxicity of the atmospheric reaction product 2-nitronaphthalene in human lymphoblastoid cell lines, Mutat. Res. 445 (1999) 113–125.
[13] G.M. Conzelman Jr., J.E. Moulton, L.E. Flanders III, Tumors in the urinary bladder of a monkey: induction with 2-nitronaphthalene, Gann 61 (1970) 79–80.
[14] A. Delgado-Rodriguez, R. Ortiz-Marttelo, U. Graf, R. Villalobos-Pietrini, S. Gomez-Arroyo, Genotoxic activity of environmentally important polycyclic aromatic hydrocarbons and their nitro derivatives in the wing spot test of *Drosophila melanogaster*, Mutat. Res. 341 (1995) 235–247.
[15] R.E. Rasmussen, D.H. Do, T.S. Kim, L.C. Dearden, Comparative cytotoxicity of naphthalene and its monomethyl- and mononitro-derivatives in the mouse lung, J. Appl. Toxicol. 6 (1986) 13–20.
[16] R. Paige, V. Wong, C. Plopper, Dose-related airway-selective epithelial toxicity of 1-nitronaphthalene in rats, Toxicol. Appl. Pharmacol. 147 (1997) 224–233.
[17] J.-M. Sauer, R.R. Eversole, C.L. Lehmann, D.E. Johnson, L.J. Beuving, An ultrastructural evaluation of acute 1-nitronaphthalene induced hepatic and pulmonary toxicity in the rat, Toxicol. Lett. 90 (1997) 19–27.
[18] J. Sasaki, S.M. Aschmann, E.S.C. Kwok, R. Atkinson, J. Arey, Products of the gas-phase OH and NO_3 radical-initiated reactions of naphthalene, Environ. Sci. Technol. 31 (1997) 3173–3179.
[19] J. Arey, Atmospheric reactions of PAHs including formation of nitroarenes, in: A.H. Neilson (Ed.), The Handbook of Environmental Chemistry: PAHs and Related Compounds, vol. 3, Part I, Springer, Berlin, 1998, pp. 347–385.
[20] M.G. Nishioka, B. Petersen, J. Lewtas, Comparison of nitro-aromatic content and direct-acting mutagenicity of passenger car engine emissions, in: D. Rondia, M. Cooke, R.K. Haroz (Eds.), Mobile Source Emissions Including Polycyclic Organic Species, Reidel, Dordrecht, 1983, pp. 197–210.
[21] M.C. Paputa-Peck, R.S. Marano, D. Schuetzle, T.L. Riley, C.V. Hampton, T.J. Prater, L.M. Skewes, T.E. Jensen, Determination of nitrated polynuclear aromatic hydrocarbons in particulate extracts by capillary column gas chromatography with nitrogen selective detection, Anal. Chem. 55 (1983) 1946–1954.
[22] D. Schuetzle, M. Paputa, C.M. Hampton, R. Marano, T. Riley, T.J. Prater, L. Skewes, I. Salmeen, The identification and potential sources of nitrated polynuclear aromatic hydrocarbons (nitro-PAH) in diesel particulate extracts, in: D. Rondia, M. Cooke, R.K. Haroz (Eds.), Mobile Source Emissions Including Polycyclic Organic Species, Reidel, Dordrecht, 1983, pp. 299–312.
[23] W.C. Yu, D.H. Fine, K.S. Chiu, K. Biemann, Determination of nitrated polycyclic aromatic hydrocarbons in diesel particulates by gas chromatography with chemiluminescent detection, Anal. Chem. 56 (1984) 1158–1162.
[24] A. Feilberg, R.M. Kamens, M.R. Strommen, T. Nielsen, Modeling the formation, decay, and partitioning of semivolatile nitro-polycyclic aromatic hydrocarbons (nitronaphthalenes) in the atmosphere, Atmos. Environ. 33 (1999) 1231–1243.
[25] R. Atkinson, J. Arey, A.M. Winer, B. Zielinska, A survey of ambient concentrations of selected polycyclic aromatic hydrocarbons (PAHs) at various locations in California, Final Report to California Air Resources Board Contract no. A5-185-32, Sacramento, CA, 1988.
[26] J. Arey, B. Zielinska, R. Atkinson, A.M. Winer, Polycyclic aromatic hydrocarbon and nitroarene concentrations in ambient air during a wintertime high-NO_x episode in the Los Angeles basin (California, USA), Atmos. Environ. 21 (1987) 1437–1444.
[27] R. Atkinson, J. Arey, M.C. Dodge, W.P. Harger, P. McElroy, P.T. Phousongphouang, Yields and reactions of intermediate compounds formed from the initial atmospheric reactions of selected VOCs, Final Report to California Air Resources Board Contract no. 96-306, Sacramento, CA, 2001.
[28] R. Atkinson, S.M. Aschmann, J. Arey, B. Zielinska, D. Schuetzle, Gas-phase atmospheric chemistry of 1- and 2-nitronaphthalene and 1,4-naphthoquinone, Atmos. Environ. 23 (1989) 2679–2690.
[29] J. Arey, R. Atkinson, S.M. Aschmann, D. Schuetzle, Experimental investigation of the atmospheric chemistry of 2-methyl-1-nitronaphthalene and a comparison of predicted nitroarene concentrations with ambient air data, Polycyclic Aromat. Compd. 1 (1990) 33–50.
[30] Z. Fan, R.M. Kamens, J. Zhang, J. Hu, Ozone–nitrogen dioxide–NPAH heterogeneous soot particle reactions and modeling NPAH in the atmosphere, Environ. Sci. Technol. 30 (1996) 2821–2827.
[31] B. Zielinska, J. Arey, R. Atkinson, T. Ramdahl, A.M. Winer, J.N. Pitts Jr., Reaction of dinitrogen pentoxide with fluoranthene, J. Am. Chem. Soc. 108 (1986) 4126–4132.
[32] J. Arey, B. Zielinska, High resolution gas chromatography/mass spectrometry analysis of the environmental pollutants methylnitronaphthalenes, J. High Resolut. Chromatogr. 12 (1989) 101–105.
[33] L. Zafonte, P.L. Rieger, J.R. Holmes, Nitrogen dioxide photolysis in the Los Angeles atmosphere, Environ. Sci. Technol. 11 (1977) 483–487.
[34] A. Feilberg, R.M. Kamens, M.R. Strommen, T. Nielsen, Photochemistry and partitioning of semivolatile nitro-PAH in the atmosphere, Polycyclic Aromat. Compd. 14–15 (1999) 151–160.
[35] J.C. Calvert, R. Atkinson, K.H. Becker, R.M. Kamens, J.H. Seinfeld, T.J. Wallington, G. Yarwood, Primary photochemical processes of the aromatic hydrocarbons and some their common oxidation products, in: The Mechanisms of Atmospheric Oxidation of Aromatic Hydrocarbons, Chapter VII, Oxford University Press, New York, NY, 2002, pp. 230–310.
[36] O.L. Chapman, A.A. Griswold, E. Hoganson, G. Lenz, J. Reasoner, Photochemistry of unsaturated nitrocompounds, J. Pure Appl. Chem. 9 (1964) 585–590.
[37] O.L. Chapman, D.C. Heckert, J.W. Reasoner, S.P. Thackaberry, Photochemical studies on 9-nitroanthracene, J. Am. Chem. Soc. 88 (1966) 5550–5554.
[38] A.M. van den Braken-van Leersum, C. Tintel, M. van't Zelfde, J. Cornelisse, J. Lugtenburg, Spectroscopic and photochemical properties of mononitropyrenes, Recl. Trav. Chim. Pays-Bas 106 (1987) 120–128.
[39] D. Dopp, Photochemical reactivity of the nitro group, in: W.M. Horspool, P.-S. Song (Eds.), CRC Handbook of Organic Photochemistry and Photobiology, CRC Press, Boca Raton, 1995, pp. 1019–1062.
[40] J.H. Beynon, B.E. Job, A.E. Williams, Mass spectrometry: the elimination of CO from substituted nitronaphthalenes, Z. Naturforschg. 21 (1966) 210–213.
[41] S.-T. Lin, Y.-F. Jih, P.P. Fu, Mass spectral analysis of nitropolycyclic aromatic hydrocarbons with torsion angle obtained from semiempirical calculations, J. Org. Chem. 61 (1996) 5271–5273.
[42] J. Yinon, Mass spectral fragmentation processes in nitronaphthalenes. A study using tandem mass spectrometry and collision-induced dissociation, Rapid Commun. Mass Spectrom. 7 (1993) 67–70.
[43] D.W. Miller, F.F. Evans, P.P. Fu, Effect of a nitro group geometry on the proton NMR chemical shifts of nitro aromatics, Spectrosc. Int. J. 4 (1985) 91–94.

[44] P.R. Wells, P.G.E. Alcorn, Proton magnetic resonance spectra of nitronaphthalenes in dimethylacetamide solution, Aust. J. Chem. 16 (1963) 1108–1118.

[45] E.S.C. Kwok, R. Atkinson, Estimation of hydroxyl radical reaction rate constants for gas-phase organic compounds using a structure–reactivity relationship: an update, Atmos. Environ. 29 (1995) 1685–1695.

[46] D. Yaffe, Y. Cohen, J. Arey, A.J. Grosovsky, Multimedia analysis of PAHs and nitro-PAH daughter products in the Los Angeles basin, Risk Anal. 21 (2001) 275–294.

[47] R. Kamens, J. Odum, Z.-H. Fan, Some observations on times to equilibrium for semivolatile polycyclic aromatic hydrocarbons, Environ. Sci. Technol. 29 (1995) 43–50.